Nitric oxide synergistic microwave via amplification of immunogenic cell death for enhanced tumor thermotherapy

Wenna Guo [1,2,3], Zengzhen Chen [2,3], Deen Gu [1*] and Xianwei Meng[2,3*]

[1]School of Optoelectronic Science and Engineering University of Electronic Science and Technology of China, Chengdu, Sichuan 610054, P. R. China
[2]State Key Laboratory of Cryogenic Science and Technology, Technical Institute of Physics and Chemistry, Chinese Academy of Sciences, Beijing 100190, China
[3]Laboratory of Controllable Preparation and Application of Nanomaterials, Technical Institute of Physics and Chemistry, Chinese Academy of Sciences, Beijing, 100190, China

Abstract. In recent years, microwave thermotherapy (MWT) has been widely concerned in tumor treatment. However, problems such as easy recurrence have restricted its application. And some studies have shown that thermotherapy will enhance the immune effect at the same time, but the effect is weak and not enough to inhibit tumor recurrence after thermotherapy. Therefore, we can effectively inhibit tumor growth and recurrence by enhancing the immune effect after thermotherapy. In this paper, Zr-MOF nanoparticles were used to encapsulate the donor of nitrosocysteine (CSNO) for nitric oxide release, and then the mitochondria-targeting ligand of triphenylphosphine (TPP) was attached to obtain CSNO@Zr-MOF-TPP (SZMT) nanocomposites. Under microwave irradiation, SZMT releases NO, which promotes high mobility group box 1 (HMGB1) release and calreticulin (CRT) expression, thereby activating the immune effect. The SZMT nanocomposites realizes the combined treatment of MWT, gas therapy and immunotherapy under microwave irradiation, which provides a new insight for the application of MWT in the clinic.

1. Introduction

Microwave thermotherapy (MWT) is one of the applications of MW in the field of biomedicine, which has the advantages of non-invasive, small trauma and large penetration depth [1-2]. The principle of MWT is that when microwaves penetrate into biological tissues, the biological tissues will absorb the energy of MW, which will be converted into thermal effect and warm up the tissues [3-4]. Compared with other thermotherapy techniques, MWT has the advantages of larger heating volume, faster heating speed, and higher internal heating of tissues, which is considered as the most promising thermotherapy method [5]. However, MWT cannot specifically identify tumors, and is prone to damage normal tissues around tumors during treatment, or there is a risk of residual and metastasis due to insufficient treatment resulting in incomplete killing of the tumor [6-8].

Nitric oxide (NO) has been identified as a key factor in tumor phenotype. Its intracellular levels are closely related to tumor progression and suppression [9-10]. High levels of NO interfere with cellular energy supply by damaging cellular mitochondria, which in turn inhibits tumor growth [11-12]. It has been shown that NO can restructure the tumor immunosuppressive microenvironment. It enhances immunity by suppressing regulatory T cells and improving the survival and differentiation of cytotoxic T cells [13-15]. Therefore, NO is expected to improve the problem of metastasis and recurrence after thermotherapy. However, the non-specific systemic release of NO may cause unsatisfactory reactions such as increased heart rate, decreased blood pressure, and even toxic side effects [16]. Moreover, NO is gaseous and has an extremely short half-life, which limits its use as a therapeutic agent. Therefore, precisely achieving delivery and slow release of NO within tumor cells is a severe test. Several NO donors have been used for controlled release and storage, including nitrosocysteine (CSNO), N-diazoimidazole salts N-dinitro-1,4-phenylenediamine, S-nitrosothiols, nitroglycerin, and others [17-19]. Among them, CSNO, as an endogenous species, is more suitable for delivering NO *in vivo* than other donors [20]. However, the short half-life of CSNO in blood and its insufficient accumulation in tumor tissues greatly limit its in vivo application.

Based on the above problems, we synthesized Zr-MOF nanoparticles as carriers to encapsulate CSNO, and then attached the triphenylphosphine (TPP) to obtain CSNO@ Zr-MOF-TPP (SZMT) nanocomposites, which realized the precise delivery of CSNO into the tumor tissue. Under the irradiation of microwave, the S-NO bond of CSNO broke the chain and generated NO. On the one hand, NO destroyed the cellular mitochondria, altered the mitochondrial membrane potential and blocked the cellular energy supply. On the other hand, NO can promote CRT exposure and HMGB1 release, enhance the immune effect, and reduce the metastatic and recurrence

* Corresponding author: gudeen@uestc.edu.cn (Deen Gu), mengxw@mail.ipc.ac.cn (Xianwei Meng)

of tumors after MWT. The excellent therapeutic effect under the synergistic treatment of microwave and NO was verified by *in vitro* experiments. This nanocomposite + microwave treatment system provided strong evidence for NO synergistic MWT to enhance immunogenic cell death (ICD).

2. Results and discussion

2.1. Synthesis and characterisation of SZMT nanocomposites

In this paper, Zr-MOF (ZF) nanoparticles were synthesised using a hydrothermal method, and then CSNO@Zr-MOF-TPP (SZMT) nanocomposites were synthesized on the basis of Zr-MOF by pumping, filtration, and stirring. From the scanning electron microscopy (SEM) image, we can see that the Zr-MOF nanoparticles were spherical particles with uniform size (Fig. 1a). The transmission electron microscopy (TEM) image also showed the spherical morphology of Zr-MOF nanoparticles with size around 100 nm. Figure c showed the elemental analysis of Zr-MOF nanoparticles, from which it can be seen that the Zr-MOF nanoparticles were composed of three elements, Zr, O, and N. The Zr-MOF nanoparticles had a uniform size. The average hydrated particle size of Zr-MOF nanoparticles was proved to be 187 nm by dynamic light scattering. As such, the successful synthesis of Zr-MOF nanoparticles has been validated from multiple aspects such as particle size, mapping, and morphology.

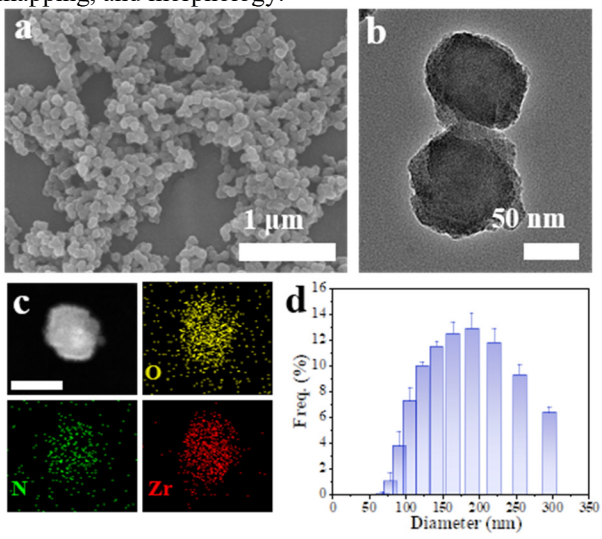

Fig. 1. Basic characterisation of ZF nanoparticles. (a) SEM of ZF nanoparticles. (b) TEM of ZF nanoparticles. (c) Mapping diagram of ZF nanoparticles. (d) Hydrated particle size map of ZF nanoparticles.

2.2. Microwave thermal conversion performance of SZMT nanocomposites

MWT limits its therapeutic effect due to poorly selective and unsignificant thermal effect. Therefore, the design and development of new microwave thermosensitizing materials has become a new orientation. It can well improve the therapeutic efficacy of MWT. Here, SZMT nanocomposites were used as microwave sensitizers and their microwave thermal conversion ability was experimentally verified. SZMT nanocomposites of different quality were divided into four groups and dissolved in 0.9 % saline. The mass consistencies were 0 mg mL^{-1}, 3 mg mL^{-1}, 5 mg mL^{-1}, and 10 mg mL^{-1}, respectively. The real-time recorded warming values showed that the experimental group with the addition of SZMT nanocomposites had a more pronounced warming effect than the control group with saline alone (Fig. 2a). When the mass consistency of ZF nanoparticles was 3 mg mL^{-1}, 5 mg mL^{-1}, and 10 mg mL^{-1}, the temperature was elevated by 1.1 ℃, 5.2 ℃, and 7.5 ℃, respectively, compared with that of saline (Fig. 2b, c). From the experimental results, it can be seen that the SZMT nanocomposites have outstanding heat transform ability, which can be applied in MWT to improve the thermotherapeutic efficacy and achieve better therapeutic goals.

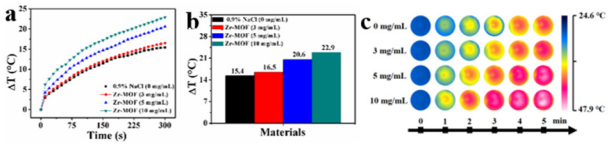

Fig. 2. (a) Plot of in vitro thermal effect evaluation of SZMT nanocomposites. (b) Temperature difference diagram for in vitro thermal effect evaluation of SZMT nanocomposites. (c) Assessment of thermal effect of SZMT nanocomposites in vitro thermal exothermogram.

2.3. Release of NO under microwave action

The SZMT nanocomposites were decentralised in PBS (pH=5.7). The tubes were centrifuged at 1, 2, 4 and 6 h to collect the supernatant. Then PBS was reintroduced and microwaved for 5 min at 1.8 W. The NO concentration in the suspension was tested by Griss reagent to come the *in vitro* release of NO from SZMT nanocomposites.

As shown in Fig. 3a, the SZMT nanocomposites released NO in an acidic environment, while the production of NO increased significantly after microwave stimulation, which was attributed to the fact that the microwave caused the cleft of the S-NO bond in the CSNO, which resulted in the emergence of a large quantity of NO. The luminous intensity of NO in the SZMT nanocomposites after the incubation of the 4T1 cells under distinctive conditions was observed by fluorescence microscopy (Fig. 3b), which also showed that the SZMT nanocomposite incubated with the 4T1 cells under different conditions had a significant increase in the generation of NO. Therefore, SZMT nanocomposite incubated 4T1 cells with considerably greater NO concentration than the comparison group after microwave stimulation.

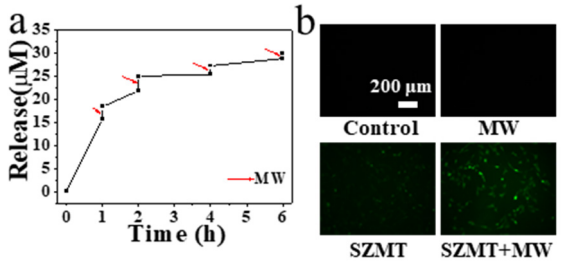

Fig. 3. (a) *In vitro* controlled release results of NO from SZMT nanocomposites. (b) Immunofluorescence map of nitric oxide in 4T1 cells.

2.4. Toxicological of SZMT nanocomposites and *in vitro* therapeutic tests

In this work, we used L929 and 4T1 to assess the biotoxicity of SZMT nanocomposites by MTT assay. The both types of cells were uniformly passed into 96-well plates, different mass consistency of SZMT nanocomposites were acceded to 96-well plate after 24 h. The SZMT nanocomposites mass consistency were 0 μg mL^{-1}, 12.5 μg mL^{-1}, 25 μg mL^{-1}, 50 μg mL^{-1}, 100 μg mL^{-1}, and 200 μg mL^{-1}, respectively. Cultivation was continued for 24 h after the addition of the material, and then 20 μL of MTT was acceded to each well, all the culture medium was added to remove the culture solution after 4 h, and 200 μL of DMSO was added. The absorbance at 492 nm of the 96-well plate was tested by using an enzyme labelling equipment to assess the survival of the cells.

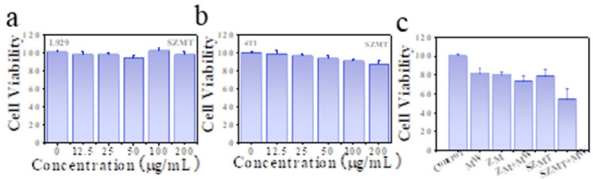

Fig. 4. (a) Biosafety estimation of SZMT nanocomposites in L929 cells. (b) Biosafety evaluation of SZMT nanocomposites in 4T1 cells. (c) Therapeutic effect of each group in 4T1 cells.

From Fig. 4a, b, it can be seen that, when the mass consistency of SZMT nanocomposites was 200 μg mL^{-1}, the viability of L929 cells was 97.48%, and that of 4T1 cells was 87.1%. These results indicated that SZMT nanocomposites have high biological safety and were suitable for in vivo therapeutic. Next, 4T1 cells were used to validate the *in vitro* effectiveness of treatment of SZMT nanocomposites. From Fig. 4c, it can be seen that the treatment effect of the simple microwave group, the ZF nanoparticle and the SZMT nanocomposite material group were not statistically significant, and the cell viability rate was about 80%. The cell survival rate in the Zr-MOF + microwave group was 73.47%, which was 7.91% lower than that in the microwave group. In SZMT + microwave group, after microwave irradiation, a large number of NO release in cell mitochondria, which would kill a large amount of cancer cells, therefore the treatment effect was obvious, and the viability rate was only 54.81%. This results of *in vivo* therapeutic experiment proved that the SZMT + microwave group had superior therapeutic effect compared with other treatment groups.

2.5. The role of NO on mitochondria

After that, 4T1 cells were passed down into 12-well plates. The experiments were divided into 4 groups, namely, control group, microwave group, SZMT group, SZMT + microwave group, and the mass concentrations of SZMT nanocomposites was 100 μg/mL. After adding the materials and continuing the incubation for 24 h, the experimental group requiring microwave was microwaved with a power of 1.8 W and the microwave time was 5 minutes. Then, the incubation was carried out using the fluorescence probe (JC-1 assay kit) for mitochondrial membrane potential. Next, we used fluorescence microscopy to observe the fluorescence effect of each group.

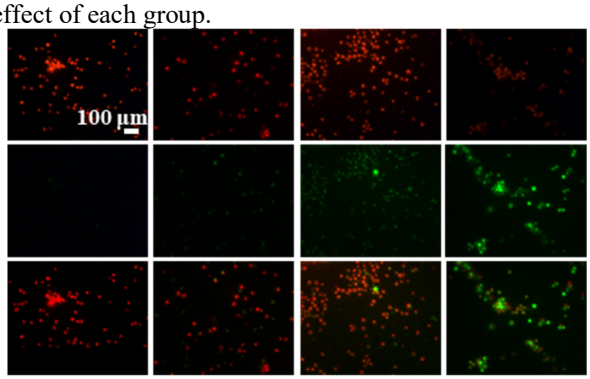

Fig. 5. Changes in mitochondrial membrane potential after treatment of 4T1 cells with MW, SZMT, and SZMT + MW.

As known from Fig. 5, the monomers of the SZMT +MW group had a intense green fluorescent intensity, whereas the aggregates of the microwave group, the SZMT and the control group had a strong red fluorescence intensity. Formation of the JC-1 monomers indicated the depolarisation of the mitochondrial membrane, demonstrating that NO induced mitochondrial dysfunction.

2.6. *In vitro* ICD activation validation

Nitric oxide (NO) has been shown to induce effective ICD effects. The ICD of tumor cells is characterized by inducing extracellular release of HMGB1 as a "find me" signal and inducing cell surface exposure of CRT as a "eat me" signal. Herein, the ability of SZMT nanocomposites to induce ICD was determined by fluorescence microscopy to detect CRT exposure and HMGB1 release.

As known from Fig. 6a, the CRT's of the control group had no fluorescence, and the fluorescent intensity of the MW and SZMT nanocomposites groups was enhanced compared to the control group, but it was still unsatisfactory. Whereas, after the combined effect of SZMT nanocomposites and microwaves, the fluorescence of CRT's was significantly enhanced. Similarly, as shown in Fig. 6b, the fluorescence effect of HMGB1 was the strongest in the control group, and the fluorescence of MW and SZMT nanocomposites groups decreased

compared with the control group, whereas the fluorescence effect of HMGB1 was almost invisible after the combined effect of SZMT nanocomposites and microwaves. Therefore, the ability of SZMT nanocomposites to induce ICD can be demonstrated by observing CRT exposure and HMGB1 release by fluorescence microscopy, which proves the ability of SZMT nanocomposites to induce ICD through the continuous release of NO under the effect of microwaves.

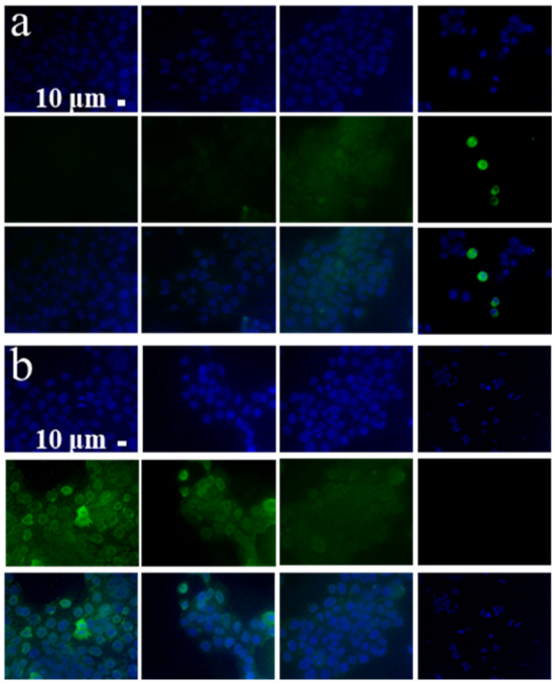

Fig. 6. (a) Immunofluorescence plots of CRT changes after treatment of 4T1 cells by MW, SZMT, and SZMT + MW. (b) Immunofluorescence plots of HMGB1 changes after treatment of 4T1 cells by MW, SZMT, SZMT + MW.

3. Conclusion

In conclusion, we synthesized Zr-MOF nanoparticles as carriers to encapsulate CSNO, and then attached the mitochondria-targeting ligand triphenylphosphine (TPP) to obtain CSNO@ Zr-MOF-TPP (SZMT) nanocomposites. It was achieved that after precise delivery of CSNO into the tumor tissue under microwave irradiation, the S-NO bond of CSNO broke the chain and generated NO. On the one hand, NO destroyed the cellular mitochondria, altered the mitochondrial membrane potential and blocked the cellular energy supply. On the other hand, NO promoted CRT exposure and HMGB1 release, enhanced the immune effect, and can reduce metastatic recurrence of tumors after MWT. The cell survival rate of 54.81% under the synergistic treatment of microwave with NO was verified by in vitro experiments. This nanocomposites + microwave therapeutic system is expected to provide hope for the clinical of MWT.

Acknowledgments

This work was supported by Beijing Natural Science Foundation (4244112), China Postdoctoral Science Foundation (2023M743599), and Postdoctoral Fellowship Program of CPSF (GZC20232772), and National Natural Science Foundation of China (62274021).

References

1. S. Li, Z. Chen, L. Tan, Q. Wu, X. Ren, C. Fu,M. Niu, H. Li, X. Meng, Biomaterials **283**, 121472 (2022)
2. W. Guo, Z. Chen, L. Tan, D. Gu, X. Ren, C. Fu, Q. Wu, X. Meng, VIEW, **3** 20200174 (2021)
3. C. Fu, H. Zhou, L. Tan, Z. Huang, Q. Wu, X. Ren, J. Ren, X. Meng, ACS Nano **12**, 2201 (2018)
4. S. Dong, Y. Dong, Z. Zhao, J. Liu, S. Liu, L. Feng, F. He, S. Gai, Y. Xie, P. Yang, J. Am. Chem. Soc. **145**, 9488 (2023)
5. W. Guo, Z. Chen, Q. Wu, L. Tan, X. Ren, C. Fu, F. Cao, D. Gu, X. Meng, Small **19**, 2308055 (2023)
6. E. A. Pietila, J. Gonzalez-Molina, L.Moyano-Galceran, S. Jamalzadeh, K. Zhang, L. Lehtinen, S. P. Turunen, T. A. Martins, O. Gultekin, T. Lamminen, K. Kaipio, U. Joneborg, J. Hynninen, S. Hietanen, S. Grenman, R. Lehtonen, S. Hautaniemi, O. Carpen, J. W. Carlson, K. Lehti, Nat. Commun. **12**, 3904 (2021)
7. S. Li, C. Zhu, X. Zhou, L. Chen, X. Bo, Y. Shen, X. Guan, X. Han, D. Shan, L. Sun, Y. Chen, H. Xu, W. Yue, Adv. Sci. **9**, 2104619 (2022)
8. W. Guo, M. Niu, Z. Chen, Q. Wu, L. Tan, X. Ren, C. Fu, J. Ren, D. Gu, X. Meng, Adv. Healthcare Mater. **11**, e2201441(2022)
9. J. An, Y. G. Hu, C. Li, X. L. Hou, K. Cheng, B. Zhang, R. Y. Zhang, D. Y. Li, S. J. Liu, B. Liu, D. Zhu, Y. D. Zhao, Biomaterials **230**, 119636 (2020)
10. H. Wu, D. Zhong, Z. Zhang, Y. Wu, Y. Li, H. Mao, K. Luo, D. Kong, Q. Gong, Z. Gu, ACS Nano **15**, 4845 (2021)
11. Z. Fang, J. Zhang, Z. Shi, L. Wang, Y. Liu, J. Wang, J. Jiang, D. Yang, H. Bai, B. Peng, H.Wang, X. Huang, J. Li, L. Li,W. Huang, Adv. Mater. **35**, 2301901 (2023)
12. Z. Wang, A. Jin, Z. Yang, W. Huang, ACS Nano **17**, 8935 (2023)
13. W. Jiang,W. Dong, M. Li, Z. Guo, Q. Wang, Y. Liu, Y. Bi, H. Zhou, Y. Wang, ACS Nano **16**, 3881 (2022)
14. Q. Song, G. Lan, Q. Li, Y. Lin, X. Chen, H. Liu, Y. Cheng, Y. Luan, Chem. Eng. J. **462**, 142201 (2023)
15. H. Chen, T. Li, Z. Liu, S. Tang, J. Tong, Y. Tao, Z. Zhao, N. Li, C. Mao, J. Shen, M. Wan, Nat. Commun. **14**, 941 (2023)
16. P. Liu, Y. Wang, Y. Liu, F. Tan, J. Li, N. Li, Theranostics **10**, 6774 (2020)
17. H. Hu, D. Li, W. Dai, Q. Jin, D. Wang, J. Ji, B. Z. Tang, Z. Tang, Adv. Funct. Mater. **33**, 2213134 (2023)
18. N. Liu, J. Zhu, W. Zhu, L. Chen, M. Li, J. Shen, M. Chen, Y. Wu, F. Pan, Z. Deng, Y. Liu, G. Yang, Z.

Liu, Q. Chen, Y. Yang, Adv. Mater. **35**, 2302220 (2023)

19. L. Yang, D. Wang, H. Jia, C. Yang, Y. Zhang, H. Li, J. Liu, J. Liu, Adv. Mater. **35**, 2301455 (2023).
20. Y. Fan, W. Wu, T. Luo, Y. Hu, Q. Zhang, J. Zhang, X. Xia, Chem. Commun. **57**, 12520 (2021).